

## SYNTHESIS AND CHARACTERIZATION OF GRAPHENE BASED IRON OXIDE (Fe<sub>3</sub>O<sub>4</sub>) NANOCOMPOSITES

T. Kamakshi<sup>1,3,\*</sup>, G. Sunita Sundari<sup>1</sup>, Harikrishna Erothu<sup>2,\*</sup> and T. P. Rao<sup>1</sup>

<sup>1</sup>Department of Physics, KoneruLakshmaiah Education Foundation (KLEF), Vaddeswaram, Guntur-522502, Andhra Pradesh, India.

<sup>2</sup>Center for Advanced Energy Studies (CAES), KoneruLakshmaiah Education Foundation (KLEF), Vaddeswaram, Guntur-522502, Andhra Pradesh, India.

<sup>3</sup>Department of Physics, MallaReddy Engineering College for women, Maisammaguda, Dhulapally, Secunderabad-500014, Telangana, India.

\*E-mail: kamakshi.gopavarapu@gmail.com

---

### ABSTRACT

This work reports the synthesis of iron oxide (Fe<sub>3</sub>O<sub>4</sub>) nanocomposites (NCs) such as Fe<sub>3</sub>O<sub>4</sub>/GO, Fe<sub>3</sub>O<sub>4</sub>/rGO using Co-precipitation method. The synthesized NCs were characterized by X-ray diffraction (XRD), Field emission scanning electron microscopy (FE-SEM), Fourier transforms infrared spectroscopy (FTIR), and Diffuse reflectance ultraviolet-visible spectrophotometry (DRS). The XRD analysis showed the formation of Fe<sub>3</sub>O<sub>4</sub>/rGO nanocomposite. FE-SEM images revealed that Fe<sub>3</sub>O<sub>4</sub> spherical nanoparticles are uniformly deposited on the reduced graphene oxide (rGO) sheets. FTIR confirms the formation of inverse ferrite spinel structure and DRS studies showed the strong absorption in the visible region and both types (direct and indirect) of energy bands were calculated for iron oxide (Fe<sub>3</sub>O<sub>4</sub>) NCs.

**Keywords:** Co-precipitation method, Fe<sub>3</sub>O<sub>4</sub> nanoparticles, Iron oxide nanocomposites, Structural properties, Optical properties.

© RASAYAN. All rights reserved

### INTRODUCTION

Currently graphene oxide (GO) is an emerging innovative material in the world of science and technology because of their unique and outstanding properties.<sup>1,2</sup> The water-soluble derivative of graphene oxide, is highly appreciated and continues to be intensely investigated by scientists around the world due to its unique two-dimensional lamellar structure and high surface area as well as full surface accessibility and edge reactivity.<sup>3-5</sup> GO is an allotrope of carbon contains a random distribution of oxygen-containing functional groups which are combined with the carbon atoms retain sp<sup>2</sup> hybridization. GO is cheaper and easier to manufacture than graphene and can be easily reduced to Graphene-like sheets by removing the oxygen-containing groups leads to easily to be mixed with different polymers and other materials and enhance properties like conductivity, elasticity, tensile strength and more in solid form for composite.<sup>6</sup> In recent few years, considerable attention has been devoted to metal oxides especially on Fe<sub>3</sub>O<sub>4</sub> nanoparticles because of their low cost, non-toxicity, eco-friendly and facile preparation methods. Moreover, Fe<sub>3</sub>O<sub>4</sub> nanoparticles exhibit remarkable magnetic, electrical, optical and chemical properties which enhance their response to the external magnetic field and therefore greatly facilitate the treatment of the particles in practical uses.<sup>7</sup> Graphene-based iron oxide (Fe<sub>3</sub>O<sub>4</sub>) nanocomposites can be synthesized by different methods such as hydrothermal synthesis<sup>8,9</sup>, thermal decomposition<sup>10,11</sup>, co-precipitation<sup>12,13</sup>, sol-gel method<sup>14</sup>, and colloidal chemistry method.<sup>15</sup> Among these preparation techniques, chemical co-precipitation technique has proven to be the most promising technique for the production of nanomaterials. Chemical co-precipitation technique is quite simple, cheap, the most environmentally friendly and the particles can be obtained with controlled particle size.

In the current work, our motivation is to synthesize and characterize the iron oxide nanocomposites to show their enhanced properties for numerous applications in various fields such as catalysis, water purification, capacitors, sensors, biomedical diagnosis and therapy.<sup>16,17</sup> First Fe<sub>3</sub>O<sub>4</sub> nanoparticles are synthesized through chemical co-precipitation technique.<sup>18</sup> Fe<sub>3</sub>O<sub>4</sub>-rGO nanocomposite was prepared by incorporating Fe<sub>3</sub>O<sub>4</sub> nanoparticles on the surface of reduced graphene oxide (rGO). During the reduction process, the carboxylic and epoxy groups of graphene oxide are lost, resulting in the less dispersion of the magnetic nanocomposite in water and other polar solvents<sup>7</sup>. The synthesized nanocomposites were characterized by XRD, FTIR, FE-SEM and DRS UV-VIS spectrophotometer.

## EXPERIMENTAL

### Materials

Chemical reagents such as Ferrous chloride tetrahydrate (FeCl<sub>2</sub>·4H<sub>2</sub>O, AR) purchased from Sigma Aldrich, Ferric chloride hexahydrate (LR) purchased from Dr. MACS BIO-PHARMA PRIVATE LIMITED. All other chemicals used in this work were of analytical grade and were used directly without any purification. Unless otherwise specified, Deionized water was used for all the experiments.

### Synthesis of Fe<sub>3</sub>O<sub>4</sub> Nanoparticles

Fe<sub>3</sub>O<sub>4</sub> nanoparticles were synthesized by chemical co-precipitation procedure. Typically, 2 g of FeCl<sub>2</sub>·4H<sub>2</sub>O was dissolved in 21 ml DI water and 4 ml HCl to prepare an aqueous solution (A). Further 5.4 g of FeCl<sub>3</sub>·6H<sub>2</sub>O was dissolved in 20 ml of HCl to prepare an aqueous solution (B). Solutions A and B were then mixed together at room temperature, stirred with 900 rpm and allowed to reach equilibrium for 1 hr. Then 17.5 ml ammonia (NH<sub>4</sub>OH) solution was added quickly to increase the PH value of solution which is required for the formation of Fe<sub>3</sub>O<sub>4</sub> nanoparticles<sup>10</sup>. Initially, a brown precipitate was obtained which eventually turned black as the sample continued to oxidize. Thus obtained precipitate after 30 min was washed with DI water several times with the help of a bar magnet and dried in a vacuum oven at 60 °C.

### Synthesis of Fe<sub>3</sub>O<sub>4</sub>-rGO Nanocomposite

GO was prepared according to the modified Hummer's method by oxidizing the graphite powder<sup>19</sup>. In a typical reaction to prepare Fe<sub>3</sub>O<sub>4</sub>-rGO nanocomposite, 20 g of GO was dispersed in 20 ml deionizer water by ultrasonication process for 2 hrs, to obtain a homogeneous solution, after which 5 ml HCl was added. Then 3 drops of hydrazine hydrate were added by maintaining the reaction temperature of around 80°C to 85°C and stirred for 1hr at 900 rpm. Subsequently, 5.4 g of FeCl<sub>3</sub>·6H<sub>2</sub>O was added and the stirring continued for 1hr. Then 2 g of FeCl<sub>2</sub>·4H<sub>2</sub>O was added to the mixture solution of GO and the mixture solution was stirred for 30 minutes. Finally, NH<sub>4</sub>OH solution (30 % NH<sub>4</sub>OH) dissolved in 225 ml DI water was added and stirred for 30 min. The solution turned to black<sup>20</sup>. Then the precipitate was washed several times with DI water until it reached a neutral PH = 7. The precipitate was separated and dried in a vacuum oven at 60 °C. Fe<sub>3</sub>O<sub>4</sub>-GO nanocomposite was also synthesized under similar conditions mentioned above except the addition of hydrazine hydrate.

## RESULTS AND DISCUSSION

### Structural Properties

XRD patterns of Fe<sub>3</sub>O<sub>4</sub> nanoparticles, Fe<sub>3</sub>O<sub>4</sub>-GO, and Fe<sub>3</sub>O<sub>4</sub>-rGO nanocomposites are shown in Fig.-1. The XRD pattern of Fe<sub>3</sub>O<sub>4</sub> nanoparticles shows six characteristic peaks for 2θ values of 30.26°, 35.74°, 43.22°, 53.32°, 57.24° and 62.8° corresponding to (220), (311), (400), (422), (511) and (440) Bragg reflections of face-centered cubic spinel Fe<sub>3</sub>O<sub>4</sub> structure, respectively (JCPDS no.85-1436). These characteristic peaks were also noticed in the XRD patterns of Fe<sub>3</sub>O<sub>4</sub>-GO and Fe<sub>3</sub>O<sub>4</sub>-rGO nanocomposites. No additional impurity peaks were detected in all the XRD patterns indicating the high phase purity of these cubic Fe<sub>3</sub>O<sub>4</sub> nanoparticles/nanocomposites. The diffraction patterns of composites show no structural changes in comparison with Fe<sub>3</sub>O<sub>4</sub> nanoparticles. Though the XRD patterns of nanocomposites indicated no change in the characteristic peaks, a slight change in peak intensity and width was observed<sup>21</sup>. The broad nature of peaks suggests the nano nature of all the samples. The average crystallite size was

determined from the full-width half maxima (FWHM) of the strongest reflection of the (311) peak using the Scherrer formula <sup>22</sup>.

$$D = \frac{0.9\lambda}{\beta \cos\theta} \quad (1)$$

The FWHM and average crystallite size values for all the samples are given in Table-1. The lattice parameter of the Fe<sub>3</sub>O<sub>4</sub> nanoparticles, as calculated from the XRD pattern, is found to be 8.366<sup>o</sup>Å. It is significantly lower than that of bulk material (8.396<sup>o</sup>Å). This is due to the internal atoms are compressed into the spherical entities forming the nanoparticle assembly <sup>23</sup>.

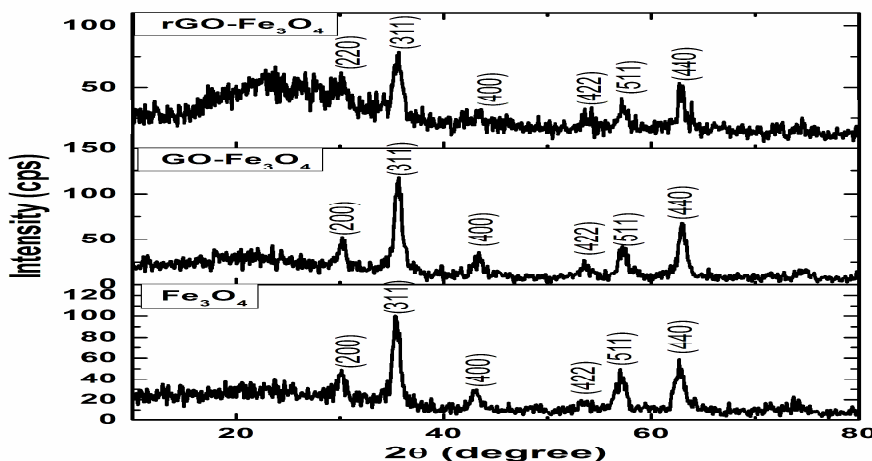


Fig.-1: XRD patterns of Fe<sub>3</sub>O<sub>4</sub> nanoparticles, Fe<sub>3</sub>O<sub>4</sub>-GO and Fe<sub>3</sub>O<sub>4</sub>-rGO nanocomposites

Table-1: Crystallite size calculated from XRD data of different samples

Sample	FWHM(degree)	Crystallite size (nm)	Lattice parameter <sup>o</sup> Å
Fe <sub>3</sub> O <sub>4</sub>	0.8	11.5	8.366
Fe <sub>3</sub> O <sub>4</sub> /GO	0.81	10.4	8.386
Fe <sub>3</sub> O <sub>4</sub> /rGO	0.83	7.82	8.403

FTIR spectra of iron oxide (Fe<sub>3</sub>O<sub>4</sub>) nanoparticles, Fe<sub>3</sub>O<sub>4</sub>-GO and Fe<sub>3</sub>O<sub>4</sub>-rGO nanocomposites are exposed in Fig.-2. The absorption peak at 562.34 cm<sup>-1</sup> pragmatic in case of Fe<sub>3</sub>O<sub>4</sub> nanoparticles belongs to the stretching mode of Fe-O bonds in Fe<sub>3</sub>O<sub>4</sub> <sup>24</sup>. The broad absorption at 3396.20 cm<sup>-1</sup> related to the O-H stretching represents the presence of hydroxyl groups that reside at the Fe<sub>3</sub>O<sub>4</sub> nanoparticles surface, the band at 1622.28 cm<sup>-1</sup> is due to the angular vibration of O-H. The manifestation of all these bands in IR spectra for all the samples can be ascribed to a surface covering by hydroxyl groups of water <sup>25,26</sup>. But the FTIR spectrum of Fe<sub>3</sub>O<sub>4</sub>-GO nanocomposite suggests that the formation of Fe<sub>3</sub>O<sub>4</sub> and GO. A broad band at 561.19 cm<sup>-1</sup> is attributed to Fe-O vibration of Fe<sub>3</sub>O<sub>4</sub>. The characteristic band of O-H stretching vibration appeared at 3410.98 cm<sup>-1</sup>, indicating that the C=O group is partially reduced to C-OH group. Whereas, FTIR spectrum of Fe<sub>3</sub>O<sub>4</sub>-rGO exhibits a peak at 1622.11 cm<sup>-1</sup> assigned to the C=C stretching vibration. This indicates that GO is totally electro reduced to rGO. The Fe-O vibration band at 561.25 cm<sup>-1</sup> also indicates the presence of Fe<sub>3</sub>O<sub>4</sub>; furthermore, it indicates that Fe<sup>+2</sup> have been oxidized into Fe<sub>3</sub>O<sub>4</sub> nanoparticles by graphene oxide <sup>27</sup>. These results specify the reduction of GO to rGO and presence of Fe<sub>3</sub>O<sub>4</sub> nanoparticles.

FE-SEM images of Fe<sub>3</sub>O<sub>4</sub> nanoparticles, Fe<sub>3</sub>O<sub>4</sub>-GO and Fe<sub>3</sub>O<sub>4</sub>-rGO nanocomposites are shown in Fig.-3. It shows that the surface of rGO sheet is uniformly and densely anchored with Fe<sub>3</sub>O<sub>4</sub> nanoparticles; thus, the perfect anchoring and uniform dispersion of Fe<sub>3</sub>O<sub>4</sub> nanoparticles on GO sheets prevent the agglomeration, which provides larger surface area; thus, facilitates the electrons transfer process <sup>28</sup>.

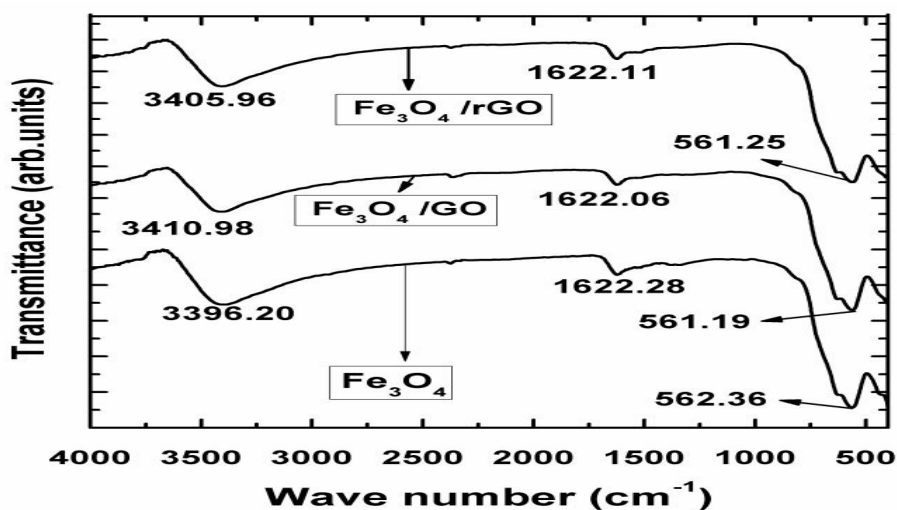


Fig.-2: FTIR spectra of  $\text{Fe}_3\text{O}_4$  nanoparticles,  $\text{Fe}_3\text{O}_4$ -GO and  $\text{Fe}_3\text{O}_4$ -rGO nanocomposites

Moreover, no independent  $\text{Fe}_3\text{O}_4$  nanoparticles outside the rGO sheets are observed, which implies that all the decorated nanoparticles are firmly attached to the surface. FE-SEM studies showed dense morphology for all samples with a uniform distribution of spherical particles.

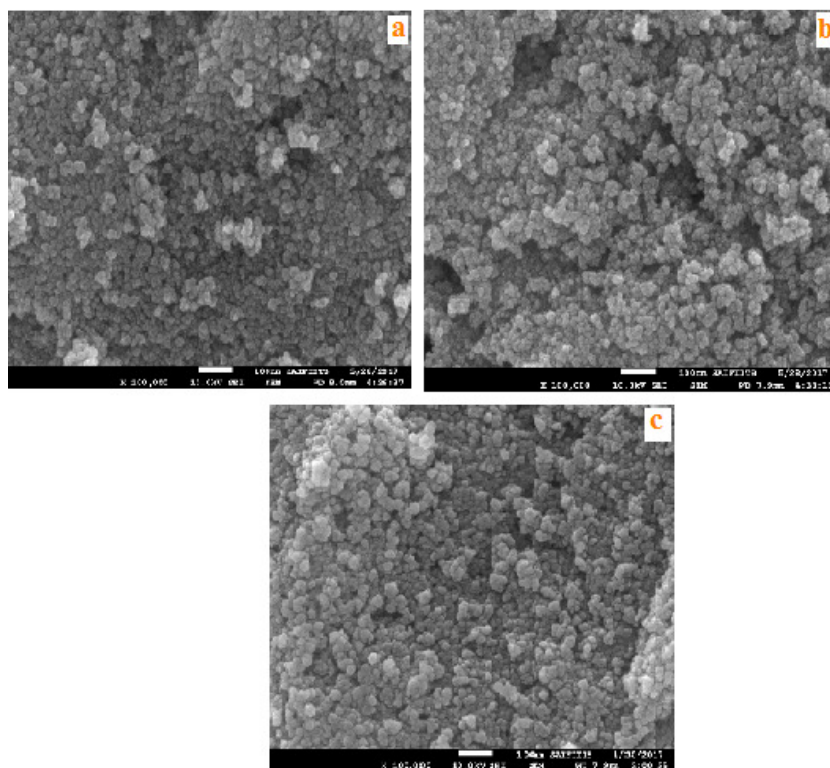


Fig.-3: FE-SEM images of (a)  $\text{Fe}_3\text{O}_4$  nanoparticles, (b)  $\text{Fe}_3\text{O}_4$ -GO and (c)  $\text{Fe}_3\text{O}_4$ -rGO nanocomposites

### Optical Properties

Diffuse reflectance ultraviolet-visible spectrophotometry (DRS) is used to determine the optical properties of the samples. Fig.-4: shows the DRS UV-Vis spectra of pure  $\text{Fe}_3\text{O}_4$  nanoparticles,  $\text{Fe}_3\text{O}_4$ -GO and  $\text{Fe}_3\text{O}_4$ -rGO nanocomposites. The sharp absorption edge observed at near band edge for all samples.

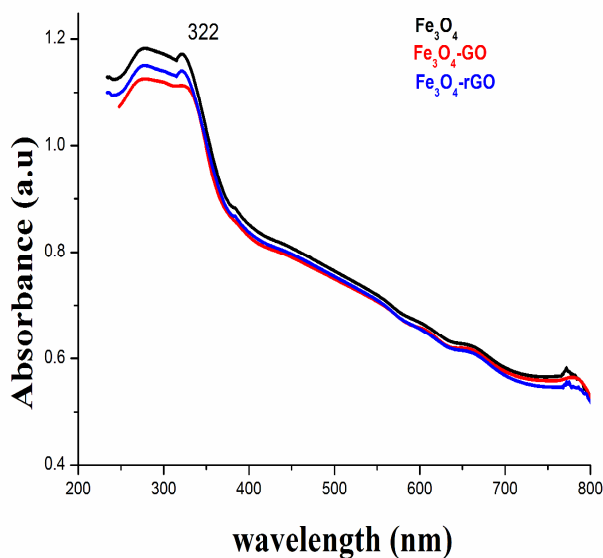


Fig.-4: UV-Vis spectra Fe<sub>3</sub>O<sub>4</sub> nanoparticles, Fe<sub>3</sub>O<sub>4</sub>-GO and Fe<sub>3</sub>O<sub>4</sub>-rGO nanocomposites

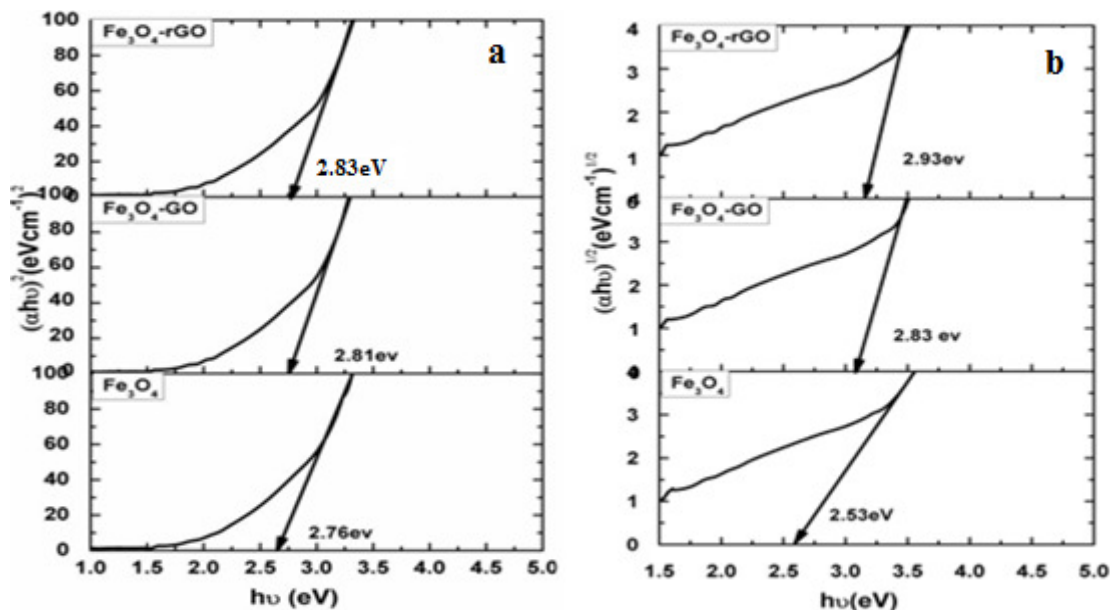


Fig.-5: (a) and (b) are Tauc plots of the Fe<sub>3</sub>O<sub>4</sub> nanoparticles and Fe<sub>3</sub>O<sub>4</sub> nanocomposites for direct indirect band gaps respectively

The band gap for the samples was calculated using the following formula <sup>29</sup> :

$$\alpha h\nu = A (h\nu - E_g)^{n/2} \tag{2}$$

Where  $\alpha$  is the absorbance,  $h$  is Planck's constant,  $\nu$  is the frequency,  $A$  is the proportion constant,  $n$  is assumed to be 1 and  $E_g$  is the band gap. Linear extrapolations are made by drawing a tangent line through the maximum slope and taking its intersection with the X-axis at  $(\alpha h\nu)^2 = 0$ . An extrapolation to  $\alpha=0$  gives an absorption energy that corresponds to the band gap. The direct and indirect band gap of the Fe<sub>3</sub>O<sub>4</sub> nanoparticles and Fe<sub>3</sub>O<sub>4</sub> nanocomposites are calculated using tauc plots and are shown in Fig.-5(a)

and (b). The direct band gap energy values of Fe<sub>3</sub>O<sub>4</sub> nanoparticles, Fe<sub>3</sub>O<sub>4</sub>-GO and Fe<sub>3</sub>O<sub>4</sub>-rGO are observed to be 2.76 eV, 2.81eV and 2.83 eV respectively. From these observations the band gap values are increased in nanocomposites due to the particle size decreases.<sup>30</sup> This leads to a shift in the absorption edge toward the high energy side which is called quantum size effect<sup>31,32</sup>. The indirect band gap of Fe<sub>3</sub>O<sub>4</sub> nanoparticles, Fe<sub>3</sub>O<sub>4</sub>-GO and Fe<sub>3</sub>O<sub>4</sub>-rGO are observed to be 2.53 eV, 2.83 eV and 2.93 eV respectively which also showed an increase in the energy band gap.

## CONCLUSION

Iron oxide (Fe<sub>3</sub>O<sub>4</sub>) nanocomposites (NCs) were successfully synthesized using the co-precipitation method. XRD pattern represented the high phase purity of cubic Fe<sub>3</sub>O<sub>4</sub> NCs. The diffraction peaks of Fe<sub>3</sub>O<sub>4</sub>-rGO composite were in good agreement with the face-centered cubic spinal structure and showed no structural changes in comparison with Fe<sub>3</sub>O<sub>4</sub> nanoparticles. FTIR spectra showed that the reduction of GO to rGO and also the presence of Fe<sub>3</sub>O<sub>4</sub> magnetic nanoparticles. Both the direct and indirect band gap energies of Fe<sub>3</sub>O<sub>4</sub> nanoparticles and Fe<sub>3</sub>O<sub>4</sub> NCs were calculated and found that the band gap energy values increased for Fe<sub>3</sub>O<sub>4</sub>-GO and Fe<sub>3</sub>O<sub>4</sub>-rGO. These results indicate that synthesized NCs enhanced their properties and these NCs can be promising materials for the applications in catalysis, water purification, etc.

## ACKNOWLEDGMENT

The authors are thankful to Prof. L.S.S Reddy (Vice-Chancellor), Dr. K. L. Narayana (Dean, R & D), and KLEF for their constant support and providing laboratory facilities for this work. The authors are also thankful to Dr. A.V. Ravindra and Dr. Ch. Rajesh, Department of physics, KLEF, for their valuable suggestions for the experimental part of this work.

## REFERENCES

1. A. K. Geim, and K. S. Novoselov, *Nature Materials.*, **6(3)**, 183(2007), DOI: 10.1038/nmat1849.
2. K. S. Novoselov, A. K. Geim, S. V. Morozov, D. Jiang, M. I. Katsnelson, I. V. Grigorieva, S. V. Dubonos, and A. A. Firsov, *Nature.*, **438(7065)**, 197(2005), DOI: 10.1038/nature04233.
3. S. Wu, S. S. A An, and J. Hulme, *Int.J.Nanomedicine.*, **10**, (2015), DOI: 10.2147/IJN.S88285.
4. H. He and C. Gao, *ACS Appl. Mater. Interfaces.*, **2**, 3201(2010), DOI: 10.1021/am100673g.
5. W. Fan, et al., *J. Mater. Chem.*, **22**, 25108(2012), DOI: 10.1039/C2JM35609K.
6. P. C. Kwan, K. Matsushita, T. Taniike and M. Terano, *Materials., Article*, (2016), DOI: 10.3390/ma9040240.
7. Poedji Loekitowati Hariani, MD. Faizal, Ridwan, Marsi, and Dedi Setiabudidaya, *Int. J. of Env. Sci. and Develop.*, **4**, (2013)
8. V. Sreeja and P.A. Joy, *Materials Research Bulletin.*, **42(8)**, 1570(2007), DOI: 10.1016/j.materresbull.2006.11.014.
9. T. J. Daou, G. Pourroy, S. B'egin-Colin, et al., *Chem. Mater.*, **18(18)**, 399(2006), DOI: 10.1021/cm060805r.
10. K. Simeonidis, S. Mourdikoudis, M. Moulla, et al., *J. Magnetism and Magnetic Materials.*, **316(2)**, e1(2007), DOI: 10.1016/j.jmmm.2008.01.028.
11. W. Zhou, K. Tang, S. Zeng, and Y. Qi, *Nanotechnology*, **19(6)**, (2008), DOI:10.1088/0957-4484/19/6/065602.
12. W. Yu, T. Zhang, J. Zhang, X. Qiao, L. Yang, and Y. Liu, *Materials Letters.*, **60(24)**, 2998(2006), DOI: 10.1155/2012/608298.
13. I. Nedkov, T. Merodiiska, L. Slavov, R.E. Vandenberghe, Y. Kusano, and J. Takada, **300(2)**, 358(2006), DOI: 10.1016/j.jmmm.2005.05.020.
14. J. Hu, G. Chen, and I. M. C. Lo, *Water Research.*,**39(18)**,4528(2005), DOI: 10.1016/j.watres.2005.05.051.
15. P. D. Cozzoli, E. Snoeck, M. A. Garcia et al., *Nano Letters.*, **6(9)**, 1966 (2006), DOI: 10.1021/nl061112c.
16. W. Guoxiu, W. Bei, P. Jinsoo, Y. Juan, S. Xiaoping, Y. Jane, *Carbon.*, **47**, 68(2009)

17. S. Jianfeng, H. Yizhe, S. Min, L. Na, M. Hongwei, Y. Mingxin, *J. Phys Chem. C.*, **114**, 1498(2010), DOI: [10.1021/jp909756r](https://doi.org/10.1021/jp909756r).
18. P. E. G. Casillas, C. A. R. Gonzalez and C. A. M. Pérez, *Intech.*, (2012), DOI: [10.1007/s11814-014-0179-z](https://doi.org/10.1007/s11814-014-0179-z).
19. Y. Yang, Y. Zhao, S. Sun, X. Zhang, L. Duan, X. Ge, W. Lü, *Materials Research Bulletin.*, **73**, 401(2016), DOI: [10.1016/j.materresbull.2015.09.032](https://doi.org/10.1016/j.materresbull.2015.09.032).
20. P. Zan, C. Yang, H. Sun, L. Zhao, Z. Lv, Y. He, *Colloids and Surfaces B: Biointerfaces.*, **145**, 208(2016), DOI: [10.1016/j.colsurfb.2016.04.049](https://doi.org/10.1016/j.colsurfb.2016.04.049).
21. N. Arsalani, H. Fattahi, M. Nazarpour, *EXPRESS Polymer Letters*, **4**, 329(2010).
22. G. Vaidyanathan, S. Sendhilnathan, R. Arulmurugan, *J. Magnetism and Magnetic Materials.*, **313** (2), 293(2007), DOI: [10.1016/j.jmmm.2007.01.010](https://doi.org/10.1016/j.jmmm.2007.01.010).
23. H. H. Z. U. Schubert (eds.), *Springer Wien Newyork.*, (1998)
24. N. Arsalani, H. Fattahi, M. Nazarpour, *Express Polymer Letters.*, **4** (6), 329(2010), DOI: [10.3144/expresspolymlett.2010.42](https://doi.org/10.3144/expresspolymlett.2010.42).
25. A. C.H. Barreto, et. al., Fechine, *Int. J. Mol. Sci.*, **14** (9), 18269(2013).
26. A. C. H. Barreto, V. R. Santiago, S.E. Mazzetto, J.C. Denardin, R. Lavín, G. Mele, M. E. N. P. Ribeiro, I. G. P. Vieira, T. Gonçalves, N. M. P. S. Ricardo, P. B. A. Fechine, *J. nanoparticle research.*, **13**, 6545(2011), DOI: [10.1007/s11051-011-0559-9](https://doi.org/10.1007/s11051-011-0559-9).
27. L. Xiong, L. Zhengz, J. Xu, W. Liu, X. Kang, Y. Wang, W. Wang, S. Yang and J. Xia, *ECS Electrochem. Letter.*, **3** (12), B26(2014), DOI: [10.1039/x0xx00000x](https://doi.org/10.1039/x0xx00000x).
28. X. Yang, X. Zhang, Y. Ma, Y. Huang, Y. Wang and Y. Chen, *J.Mater. Chem.*, **19**, 2710(2009), DOI: [10.1039/B821416F](https://doi.org/10.1039/B821416F).
29. S. Singh, R. Swarnkar, R. Gopal, *Bulletin of Materials Science*, **33**, 21(2010), DOI: [10.1007/s12034-010-0003-2](https://doi.org/10.1007/s12034-010-0003-2).
30. M. Vinothkannan, C. Karthikeyan, G. Gnanakumar, A. R. Kim, D. Jin Yoo, *Molecular and Biomolecular Spectroscopy.*, **136**, 256(2015), DOI: [10.1016/j.saa.2014.09.031](https://doi.org/10.1016/j.saa.2014.09.031).
31. S. P. im, A. Pandikumar, N. M. Huang, H. N. Lim, *Int. J. hydrogen energy.*, **39**, 14720(2014), DOI: [10.1039/C4RA09775K](https://doi.org/10.1039/C4RA09775K).
32. K. ZangenehKamali, P. Alagarsamy, N. M. Huang, B. H. Ong, H. N. Lim, *The Sci.World J.*, 396135 (2014), DOI: [10.1039/c4ra13777a](https://doi.org/10.1039/c4ra13777a).

[RJC-4003/2018]